JOTCS B
Journal of the Turkish Chemical Society
Section: B
Chemical Engineering
TURKISH CHEMICAL SOCIETY

Determining Stage Efficiency from Operating Conditions for the Liquid-Liquid Extraction Column Model Dedicated to Heavy Neutral Distillate – Aromatic Extraction Process of a Group-I Lube Base Oil Plant

Ahmet Özgür Yurdakul[1*], Suavi Noyan Kıran[2], Oğuzhan Sağlam[2], Hamide Gürnur Odabaş[2], Begüm Avcı[3]

[1]Former member, Research and Development Center, Turkish Petroleum Refineries Corporation, Kocaeli, 41790, TURKEY
[2]Process Department, İzmir Refinery, Turkish Petroleum Refineries Corporation, İzmir, 35800, TURKEY
[3]Research and Development Center, Turkish Petroleum Refineries Corporation, Kocaeli, 41790, TURKEY

Abstract: In a lube base oil production, the feed heavy neutral distillate is originated from the fractionation of various crude oil blends. Because the changing feed properties affect both yield and quality of raffinate, the plant operating conditions need to be tuned accordingly. In this study, a predictive model for an existing industrial-scale extraction process dedicated to group-I production is constructed to determine the right operating parameters in advance, which minimizes off-spec production due to faster adaption of operation to a new feedstock. It is developed via the use of the phase equilibrium data published for heavy neutral distillate + Furfural system, laboratory measurements of physical properties and composition of distillate as well as the existing plant data. The accuracy of the corresponding process model is increased via determining stage efficiency from an empirical equation based on only selected operating conditions, namely solvent temperature and solvent-to-distillate ratio.

Keywords: Lube base oil; Aromatic extraction; Furfural; Stage efficiency; Multistage column model

Submitted: May 15, 2018. **Accepted:** November 18, 2018.

Cite this: Yurdakul A, Kıran S, Sağlam O, Odabaş H, Avcı B. Determining Stage Efficiency from Operating Conditions for the Liquid-Liquid Extraction Column Model Dedicated to Heavy Neutral Distillate – Aromatic Extraction Process of a Group-I Lube Base Oil Plant. JOTCSB. 2018;2(1):13–36.

***Corresponding author**. **E-mail:** ahmetozguryur@yahoo.com.

INTRODUCTION

In the refining sector, different types of crude oils are blended and used as feed for their getting distilled, cracked, reformed and/or extracted into white products. On the other hand, the process units at a refinery are designed for a limited number of crude options. This sometimes causes asset loss due to capacity limitation or extended transient time for adapting the operation towards handling the crude mix to which the existing unit is unfamiliar. To eliminate, or at least, minimize the losses, it is important to have more information about the feed properties, and tools to predict the future response of the existing unit to the corresponding feed.

The Lube Base Oil (LBO) refinery units dedicated to Group-I production are based on Aromatic Extraction Process to alter the LBO Viscosity Index (VI) to the desired level. The essential information about the feed is aromatic content. The VI improvement is directly related to how much of this content is extracted from the oil via the use of a suitable solvent (S). This process is performed in an extraction column.

For a predictive model of column operation, the mathematical formulation of corresponding liquid-liquid extraction process is needed. In literature,

there is already available information on that, more specifically, the binary interaction parameters of the selected thermodynamic model equations (1–6). In the case that an equilibrium-based model is used, the stage efficiency (ε) information is required beside the phase equilibrium data, in order to represent the non-ideal stage behavior of a real column.

There are numerous studies assigning certain values for ε within the simulation process (7–10). In fact, it depends on certain parameters such as physico-chemical properties of corresponding liquid-liquid system, operating conditions such as temperature, pressure, flow rates, and mechanical design of column internals (11). Their effects on ε are examined at some degree (12, 13), and it is reported that it is difficult to estimate ε from these variables due to the complexity of the extraction process (14).

In this study, a novel and practical way of determining ε from only certain operating variables is defined. A predictive process model using the ε value calculated from these operational data is constructed for an existing aromatic extraction column operation. It is supported by the test-runs at which the existing plant operational data, as well as the feed/product quality information, are made available so that it becomes possible to fit an empirical equation based on only operating variables. It is used for estimating the product yield and quality against changing feed properties. The feed scope is kept to be Heavy Neutral Distillate (HND) for this model. The existing extraction column is simulated via use of Aspen Hysys. This Aspen model is supplemented with statistical models derived from the plant data and laboratory measurements. In this approach, data-driven models are integrated into first-principle ones, which can provide higher accuracy of performance prediction for a LBO extractive process.

MATERIALS AND EXPERIMENTAL METHODS

Bulk physical property and compositional measurements are performed for the distillate (D) samples prepared at the laboratory environment. Additional measurements are made for the selected physical properties of the distillate, raffinate (R) and extract (E) samples taken at the predetermined operational times during test-runs. The experimental procedures for all sample preparations and measurements are explained in this section.

Preparation of distillate samples

The D samples are prepared by mixing the raw R and E samples at different ratios in the laboratory. Here, the corresponding samples are provided from the existing LBO Unit of Tupras Izmir Refinery. Prior to mixing, they are heated up to 70 °C in a water bath till the samples get liquefied totally. It is followed by taking a portion of R sample into a beaker and weighed at a designated amount. The same procedure is applied to the E sample. Then, the R sample is poured into E, and stirred for a while to obtain a homogeneous mixture.

Bulk physical property measurements

Among the bulk physical properties of LBO, Total Sulfur, Carbon Residue, Density, Refractive Index and Kinematic Viscosity are measured for the D samples prepared in laboratory. Additionally, Density and Kinematic Viscosity measurements are performed for the D, R and E samples collected at the test-runs.

Total Sulfur: Energy Dispersive X-Ray Fluorescence (ED-XRF) is used to determine the total sulfur content. The instrument used for measurement is LAB X 3500 Oxford Instrument. Total sulfur analyses are performed according to IP 336 (15). Briefly, the sample is placed in the beam emitted from the X-Ray source, and the resultant excited characteristic X radiation is measured. The count (intensity) is compared with a calibration plot of counts against sulfur content as the percentage by mass. Series of calibration samples are prepared which cover the range of sulfur content of the sample. The concentration of sulfur in the sample from the calibration curve is measured by using the three average counts for each sample. The precision of the measurement is checked and approved according to the reproducibility limit given in IP 336.

Carbon Residue: The carbon residue content is determined according to ASTM D4530 (16), which provides an indication of the tendency to relative coke formation. Briefly, a weighed quantity of sample is placed in a glass vial and heated up to 500 °C under nitrogen atmosphere. Keeping at this temperature for a while, coking reactions occur and volatiles are swept away by nitrogen, simultaneously, and then the remaining carbonaceous-type residue is recorded as a percent of the original sample. The mass of the sample is selected according to ASTM D4530. It is not needed to distill the sample because of the high carbon residue results. 1.5 g +/- 0.5 g sample is directly placed to the carbon residue analyzer that is manufactured by PAC-Alcor. Two parallel experiments are performed for each sample. Precision and standard deviation of the results are checked according to ASTM D4530. The validated values are used for the examination at the modelling step.

Density: The density is measured according to EN

ISO 3675 (17) by using a glass hydrometer. The values are taken at the measurement temperatures and corrected to 15 °C (~60 °F) by means of a series of calculations and international standard tables. The sample is stirred via vertical and rotational motions to ensure uniform temperature and density through the hydrometer cylinder. The sufficient homogenate sample is transferred to the clean hydrometer cylinder to avoid the formation of air bubbles. The temperature of the sample is measured by a thermometer. It is recorded nearest 0.1 °C and the thermometer is removed, then the hydrometer is inserted for hydrometer scale reading. After reading, the hydrometer is carefully taken out of the fluid, and the thermometer is inserted again to read the temperature once more. The temperature value does not differ more than 0.05 °C from the previous reading. The quality of experimental data is checked according to the reproducibility calculation mentioned in EN ISO 3675.

Refractive Index: The refractive index is measured according to ASTM D1218 (18) by using a high-resolution refractometer of an automatic type with the prism temperature accurately controlled. The instrument used for measurement is KEM Refractometer RA-600. The sample is placed into the instrument, and the velocity of light passing through the sample fluid is measured. The refractive index is determined as the ratio of light velocity in the air to its velocity in the substance under examination. The precision for automatic digital refractive index procedure, as determined by the statistical examination, is checked for the quality of data. Accordingly, the values of RI analyses are at acceptable precision level.

Kinematic viscosity: The kinematic viscosity is determined according to EN ISO 3104 (19). The instrument used for measurement is Herzog HVM 472 viscometer. The time is measured for a fixed volume of sample fluid to flow down by gravity through a capillary tube. The kinematic viscosity is the product of measured flow time and the calibration constant of the viscometer. Two parallel measurements are made for the same sample, and the kinematic viscosity is taken as the average value of these two measurements as long as the values are within the reproducibility range.

Pseudo - Components Analyses:
The Clay-Gel absorption chromatographic method is used to determine the saturates (Satd), aromatics (Arom) and polar contents according to ASTM D2007 (20). The sample is percolated in n-pentane through a two-compartment column filled with clay and silica gel. Polar compounds are retained on the adsorbent clay while Arom are adsorbed on silica gel. Satd are not adsorbed on either clay or silica gel and collected from the bottom of the column.

As Polar compounds are retained in clay, this part is washed with 50% toluene-acetone mixture. Arom are recovered from silica gel via washing the corresponding part of column with toluene. The solvents (n-pentane, toluene, acetone) are completely removed away from the extracted fractions by using a rotary evaporator manufactured by IKA. The residuals are weighed and the pseudo-component contents are calculated accordingly. The quality of experimental data are checked against the reproducibility limits mentioned in ASTM D2007.

PROCESS DESCRIPTION

The solvent extraction unit (FEU) selectively extract the low viscosity aromatic components from the base oil stock by using furfural (furan-2-carbaldehyde) as the solvent. The feedstock of the unit is originated from the Vacuum Distillation Unit (VDU) or the Propane Deasphalting Unit (PDU). FEU has different operating modes according to the feedstock type, namely Spindle Oil (SO), Light Neutral (LN), Heavy Neutral (HN) and Bright Stock (BS). The first three are originated from VDU, while the last one comes from PDU. The main objective of the unit is to improve the Viscosity Index (VI) of the base oil. In addition to VI, oxidation stability and color stability targets are also met via extraction of poor quality aromatic compounds.

Solvent extraction unit can be divided into 4 groups (see Figure 1):

- Liquid-Liquid Extraction Section: It includes a Deaerator Tower and Rotating Disc Contactor (RDC). Deaerator tower strips Water and Air from the feed for further processing, since Water has an affinity to react with furfural. The deaerated feed enters from the bottom of the RDC while S enters from the top. S dissolves the aromatic components in the feed and the resultant extract is drawn from the bottom, while oil-rich R leaves from top of the column. Then, the products of RDC are sent to the related recovery sections.
- Raffinate & Extract Recovery Sections: Both include a Vacuum Flash Tower and Stripping Tower with necessary heating equipment.
- Furfural Drying Section: It includes a Fractionator and Dry Solvent Accumulator with necessary stripping units and heating equipment.

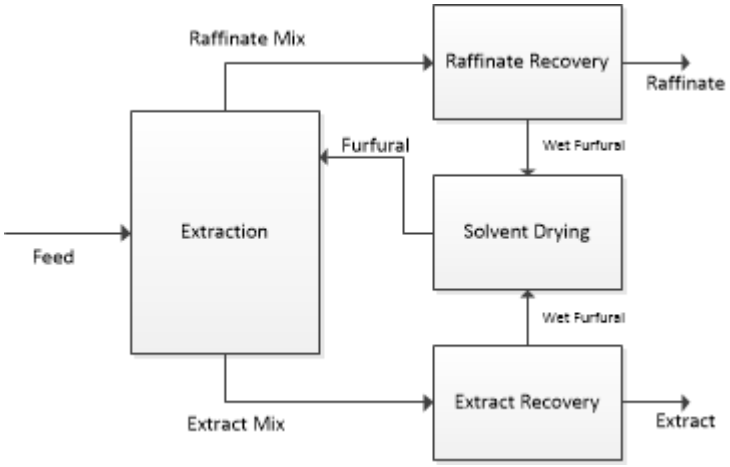

Figure 1: Solvent Extraction Unit Flowchart.

The existing Base Oil Complex is designed for Arabian light or Basra light Atmospheric Residue. The experimental crude oil is different from these.

MODEL DESCRIPTION

In the existing operation, the feed conditions are changed in daily basis due to variance in the crude mixture at the upstream. Simulating the existing extraction unit, its response to the changes in the column operating conditions, and more importantly, the bulk physical properties of the charge stream Distillate (D) can be estimated in terms of the yield and quality of the product stream R. Here, the key quality parameter for the product is Viscosity Index (VI). In the end, this model helps the Refinery Process and Planning Teams to foresee the yield and quality against changing feed conditions, which will enable better profit estimates as well as reduced amount of off-spec production during operation.

The existing industrial-scale extraction column is simulated via use of Aspen's multistage liquid-liquid extractor model. In Figure 2, the corresponding flowsheet is given. There are 3 user-defined pseudo-components representing the saturated, aromatic and polar contents of LBO. The component furfural, which corresponds to S, is also listed from the Aspen databank. The thermodynamic model is selected as NRTL for which the binary interaction coefficients published in the literature (Van Grieken et al., 2005) are used. This model is bounded to be valid for HND mode, as it is validated with the test-run data corresponding to HND. Besides NRTL parameters ae belong to Furfural extraction of HND.

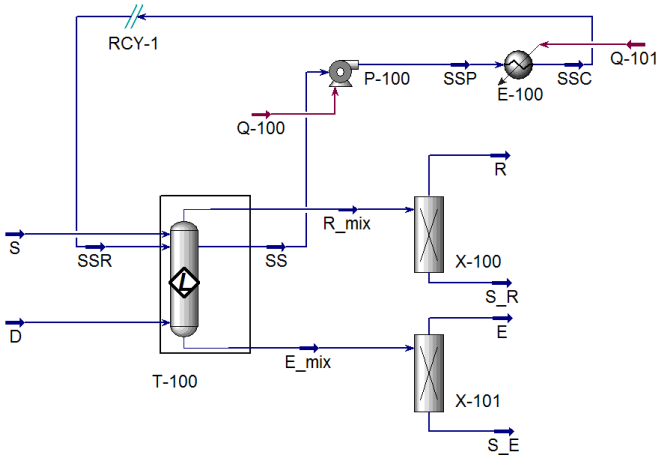

Figure 2: Aspen flowsheet of the extraction process.

In the model, D enters the column from the bottom, while S is fed from the top, representing the counter-current extraction. The bottom circulation is also added as in the case of existing unit operation. Solvent mixed R (R_mix) is taken as the top product of the column of which the bottom product is Solvent mixed Extract (E_mix). At the downstream, S is simulated to be separated from R and E at an ideal component splitter model, as the product purification and solvent

recovery are not the core parts of the operation. R and E are taken from the top of splitters.

As one of the inputs to the Aspen model, the compositional data is needed for HND, so a statistical model is developed via linear regression to predict the compositions from its bulk physical properties. The expressions for the saturated and aromatic content are given in Eqs. (1) and (2), respectively.

$$x_{Satd}^{HND} = A_{0,Satd}^{HND} + \sum A_{j,Satd}^{HND} P_j^{HND} \quad \text{(Eq. 1)}$$

Where x_{Satd}^{HND}: Saturated content of HND in mass percentage

$A_{0,Satd}^{HND}$: Intercept term for saturated content estimation

$A_{j,Satd}^{HND}$: The parameter of the jth physical property of HND for saturated content

P_j^{HND} : The jth physical property of HND

$$x_{Arom}^{HND} = A_{0,Arom}^{HND} + \sum A_{j,Arom}^{HND} P_j^{HND} \quad \text{(Eq. 2)}$$

Where x_{Arom}^{HND}: Aromatic content of HND in mass percentage

$A_{0,Arom}^{HND}$: Intercept term for aromatic content estimation

$A_{j,Arom}^{HND}$: The parameter of the jth physical property of HND for aromatic content

Here, P_j corresponds to the density at 15C (d), sulfur content (SC), carbon residue (CR), refractive index (RI), the kinematic viscosity at 80 °C (KV80), and the kinematic viscosity at 100 °C (KV100).

To create a database for pseudo-component compositions as well as bulk physical properties, HND samples are prepared in the laboratory. It is done by mixing the raw raffinate and extract samples, which are collected from the existing operation, at different ratios. For each of them, pseudo-component compositions, as well as bulk physical properties, are measured. The measurement results are listed in Table 1.

As the other input to the Aspen model, a suitable value for stage efficiency needs to be assigned. For that, an empirical equation is constructed via linear regression from the operational data of the existing unit, as shown in Eq. (3).

$$\varepsilon = A_0 + \sum A_k O_k \quad \text{(Eq. 3)}$$

Where ε: Stage efficiency

A_0: Intercept term for estimation of stage efficiency

A_k: The parameter of the kth operational data of the extraction process

O_k: The kth operational data of the extraction process

Here, O_k corresponds to operational data, i.e. Distillate Temperature (T_D), Solvent Temperature (T_S), Flow rate of Distillate (F_D), Flow rate of Solvent (F_S) and Solvent-to-Distillate Flow Ratio ($F_{S/D}$).

Test-runs are performed at the existing unit to validate the complete model. The operational data of these runs, as listed in Table 2, are used for constructing the efficiency formulation. Here, the value of ε for each run is found via data reconciliation, more specifically, iterating the FR value calculated by the Aspen model to the one realized in the corresponding run.

Table 1: The lab measurements of bulk physical properties and compositions for HND samples

Sample#	d_D	SC_D	CR_D	RI_D	$KV80_D$	$KV100_D$	$Satd_D$	$Arom_D$
1	0.941	2.32	0.73	1.499	26.5	13.9	49.31	47.47
2	0.936	2.44	0.66	1.500	24.8	13.2	47.20	37.30
3	0.901	1.34	0.20	1.478	18.6	10.6	64.00	35.30
4	0.960	3.70	1.03	1.518	32.9	16.3	36.66	58.81
5	0.964	2.76	1.11	1.520	39.0	18.6	33.29	62.99
6	0.942	2.69	0.70	1.504	28.6	14.7	45.93	51.62
7	0.944	2.31	0.71	1.505	29.2	15.0	45.59	51.77
8	0.912	1.33	0.32	1.484	21.0	11.6	35.10	54.40
9	0.989	3.73	1.68	1.535	46.1	20.9	24.73	69.80
10	0.917	2.04	0.30	1.487	21.6	11.9	57.25	38.89
11	0.933	2.17	0.61	1.497	26.1	13.8	51.89	45.35

12	0.946	1.67	0.68	1.505	31.6	15.8	47.98	48.15
13	0.948	1.81	0.74	1.503	32.4	16.0	33.80	59.50
14	0.964	2.50	1.13	1.519	38.2	18.3	34.58	61.00
15	0.951	2.25	0.92	1.511	33.2	16.5	40.49	55.66
16	0.928	1.47	0.08	1.494	25.3	13.4	51.30	41.10
17	0.987	3.66	1.64	1.535	45.4	20.6	26.85	69.67
18	0.893	0.95	0.65	1.471	17.9	10.4	70.40	15.60
19	0.942	2.33	0.86	1.503	28.3	14.6	49.65	45.49
20	0.986	3.65	1.67	1.534	44.7	20.4	27.73	66.34
21	0.964	2.95	1.15	1.516	31.9	15.9	39.67	56.36
22	0.928	1.68	0.54	1.494	25.1	13.4	56.65	39.58
23	0.932	2.14	0.58	1.497	25.9	13.7	52.01	44.04
24	0.913	1.64	0.32	1.485	20.6	11.5	63.12	33.00
25	0.915	1.53	0.26	1.485	21.8	12.0	56.54	40.70
26	0.894	1.17	0.10	1.473	17.9	10.4	74.96	23.82
27	0.904	2.20	0.19	1.478	19.2	11.0	63.22	34.89
28	0.895	1.33	0.20	1.473	18.3	10.6	71.70	26.09
29	0.891	0.94	0.13	1.470	17.5	10.2	74.69	23.52
30	0.901	1.46	0.18	1.476	18.3	10.5	70.35	27.79
31	0.899	1.32	0.10	1.475	18.7	10.8	67.10	30.88
32	0.930	2.14	0.61	1.496	25.2	13.4	51.24	44.97

Table 2: Operating conditions, reconciliation ε, realized VI and composition data calculated by the Aspen model for the test-runs performed at the existing unit

TR#*	**T_D**	**T_S**	**F_D**	**F_S**	**$F_{S/D}$**	**ε**	**$Satd_R$**	**$Arom_R$**	**VI_R**
1	96.36	131.06	85.34	170.16	1.99	0.684	78.90	21.09	116.0
2	93.49	126.95	79.97	185.70	2.32	0.670	78.92	21.07	117.7
3	92.00	127.19	80.05	192.63	2.41	0.668	78.89	21.11	118.9
4	89.18	124.49	79.90	181.71	2.27	0.640	78.90	21.10	116.7
5	100.05	123.48	79.94	189.97	2.38	0.660	78.73	21.27	118.0
6	92.43	126.93	79.92	181.45	2.27	0.659	78.92	21.08	116.0
7	94.51	126.20	80.04	182.86	2.28	0.669	78.82	21.18	118.3
8	92.67	127.48	80.00	179.00	2.24	0.670	78.20	21.29	116.3
9	92.48	127.28	80.07	172.99	2.16	0.653	78.76	21.24	113.6
10	92.99	126.49	80.06	182.32	2.28	0.662	78.72	21.28	115.3
11	95.50	127.01	80.00	183.44	2.29	0.680	78.89	21.11	114.9
12	95.97	127.79	80.00	174.25	2.18	0.667	78.79	21.21	116.6
13	95.14	128.52	79.93	179.62	2.25	0.686	78.73	21.27	115.7
14	90.01	128.31	70.00	177.11	2.53	0.691	79.20	20.80	118.8
15	90.99	128.08	69.98	175.33	2.51	0.696	78.96	21.03	117.2
16	93.15	126.79	79.93	171.08	2.14	0.664	78.66	21.34	116.2
17	94.90	127.25	79.97	171.02	2.14	0.664	78.74	21.25	118.1
18	92.56	126.51	84.90	173.92	2.05	0.683	78.65	21.34	112.9

19	93.70	124.54	79.99	169.94	2.12	0.632	78.57	21.43	116.4
20	94.74	124.16	80.02	165.31	2.07	0.613	78.45	21.55	113.5
21	95.74	124.41	80.00	168.44	2.11	0.619	78.53	21.47	115.6
22	97.36	122.77	79.97	179.75	2.25	0.627	78.41	21.58	112.9
23	96.88	125.22	80.01	162.84	2.04	0.617	78.32	21.68	114.0
24	96.07	125.90	79.97	165.34	2.07	0.627	78.64	21.36	114.7

* TR: Test-run

There are 2 Aspen model outputs from which the yield and quality data can be derived: Flow rate and composition of R. The yield (Y_R) is calculated from Eq. (4).

$$Y^R = F^R/F^D \quad \text{(Eq. 4)}$$

As the key quality parameter is not the product composition but VI of R (VI_R), the compositional data calculated for R is converted into VI information via linear regression. The empirical equation is in the form given in Eq. (5).

$$VI_R = A^R_{0,VI} + A^R_{1,VI} Satd_R + A^R_{2,VI} Arom_R \quad \text{(Eq. 5)}$$

Where VI_R: Raffinate VI

$A^R_{0,VI}$: Intercept term for estimation of VI_R

$A^R_{1,VI}$: The parameter of the saturated term for VI_R

$A^R_{2,VI}$: The parameter of the aromatic term for VI_R

The compositional and VI data from the test-runs, as listed in Table 2, are used for constructing the model. Here, the compositions are found from the corresponding operational data and physical properties of feed stream via use of the Aspen model. Besides, VI_R's are calculated from the kinematic viscosity values at 40°C (KV40) and KV100 according to ASTM D2270 (21). As the measured ones are indeed KV80 and KV100, the KV80 values need to be converted into KV40 according to the method given in ASTM D341 (22). For these transformations and calculations, the built-in software program of the viscometer is used.

Selection of the predictor variables for these 3 statistical models is discussed in the next section. Following the selection, the outliers are determined via Robust Regression. Eliminating the outliers, 75% of the operational data is used for training, and the model testing is done with the remaining 25%.

RESULTS AND DISCUSSION

Model for saturated content estimation of D

Using the data in Table 1, the linear relationship is investigated between the saturated composition and bulk physical properties of D via scattering plots, as given in Figure 3.

It is seen that the saturated content shows a smooth trend with the bulk physical properties d, RI, KV80 and KV100. As SC and CR data are rather scattered compared to the others, these are eliminated from the predictor variables. Besides, d and RI are highly correlated to each other (with Pearson product-moment correlation of 0.9970), so the only d is considered among these two to prevent bias. Together with d, the properties KV80, and KV100 are also selected as independent variables. In fact, these three selected properties require measurement time less than 1 hr, so it is also practical to use them for the prediction.

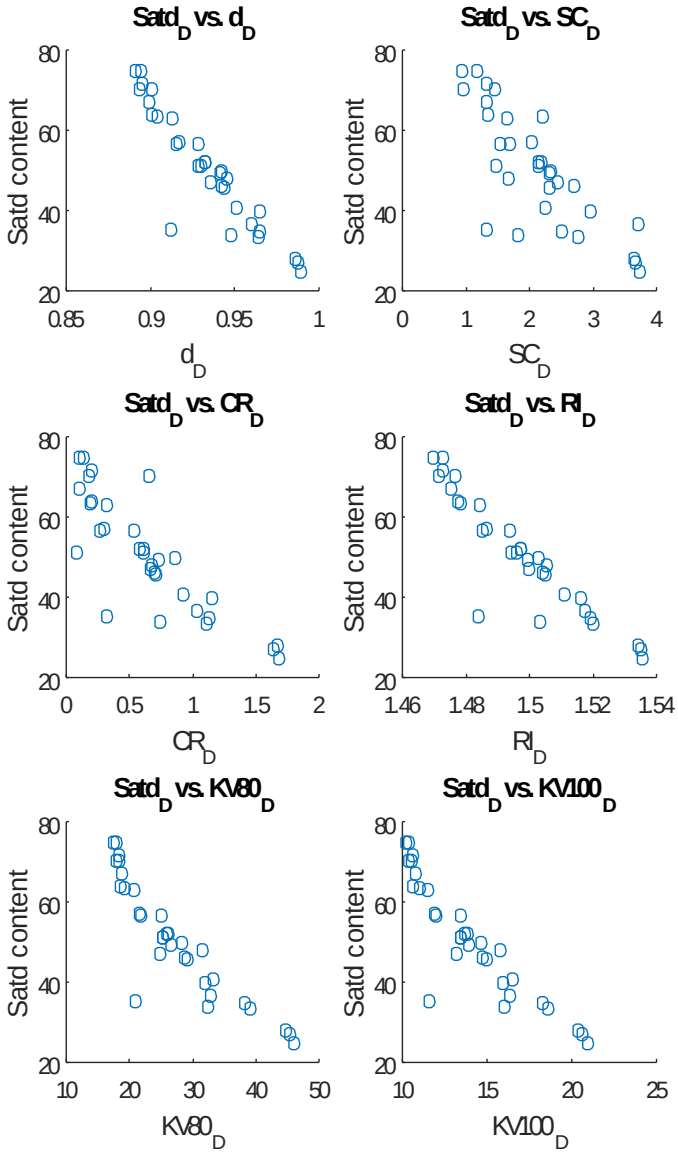

Figure 3: Scatterplots of predictor variable candidates for saturated content estimation.

Fitting a linear model with the selected predictor variables, the corresponding p-values listed in Table 3 are checked for their significance. While d_D shows its significance with a probability value lower than 0.05, KV80, and KV100 do not. It is possible that there are some outliers in the data causing this. Therefore, robust regression techniques, more specifically S estimation with 0.975 of confidence level, are applied to determine the outliers.

The outliers are found to be the 2nd, 3rd, 8th and 13th Rows. Eliminating these outliers, and using the 75% of remaining data for training, the fitting parameters are found as listed in Table 3.

Table 3: p-values for the selected bulk physical properties as predictor variables for Satd content (Values given for both complete dataset and training dataset without outliers)

	For complete dataset				For dataset without outliers			
Term	**Estimate**	**Std.Er.**	**t Ratio**	**Prob>|t|**	**Estimate**	**Std.Er.**	**t Ratio**	**Prob>|t|**
Intercept	500.92	155.1	3.23	0.0032	414.62	83.59	4.96	0.0001
d_D	-485.56	205.2	-2.37	0.0251	-336.71	111.1	-3.03	0.0075
$KV80_D$	-0.0750	2.973	-0.03	0.9800	2.9142	1.482	1.97	0.0658
$KV100_D$	0.3210	8.833	0.04	0.9713	-9.0741	4.478	-2.03	0.0587

Comparing the p-values given in Table 3, all three parameter estimates are improved after disregarding the outliers. Though the ones for KV80 and KV100 are still higher than 0.05, they are kept as the predictor variables due to the fact that the adjusted R2 increases from 0.972 to 0.975 in this case, which shows that these variables improve the model more than that would be expected by chance. Besides, one unit change of KV80 or KV100 while holding the others constant represents a non-negligible change in response. The corresponding model equation for saturated content estimation is given in Eq. (6) together with the summary of fit and ANOVA table below:

$$x_{Satd}^{HND} = 414.62 - 336.71 * d_D + 2.91 * KV80_D - 9.07 * KV100_D \quad \text{(Eq. 6)}$$

RSquare	0.979
RSquare Adj	0.975
Root Mean Square Error	2.34
Mean of Response	54.39
Observations (or Sum Wgts)	21

Source	**DF**	**Sum of Squares**	**Mean Square**	**F Ratio**
Model	3	4244.7821	1414.93	258.5350
Error	17	93.0387	5.47	**Prob >**
C. Total	20	4337.8209		<.0001

The model is tested with the remaining data. Putting the predicted and actual data, as well as the residual information in graphs, results in Figure 4.

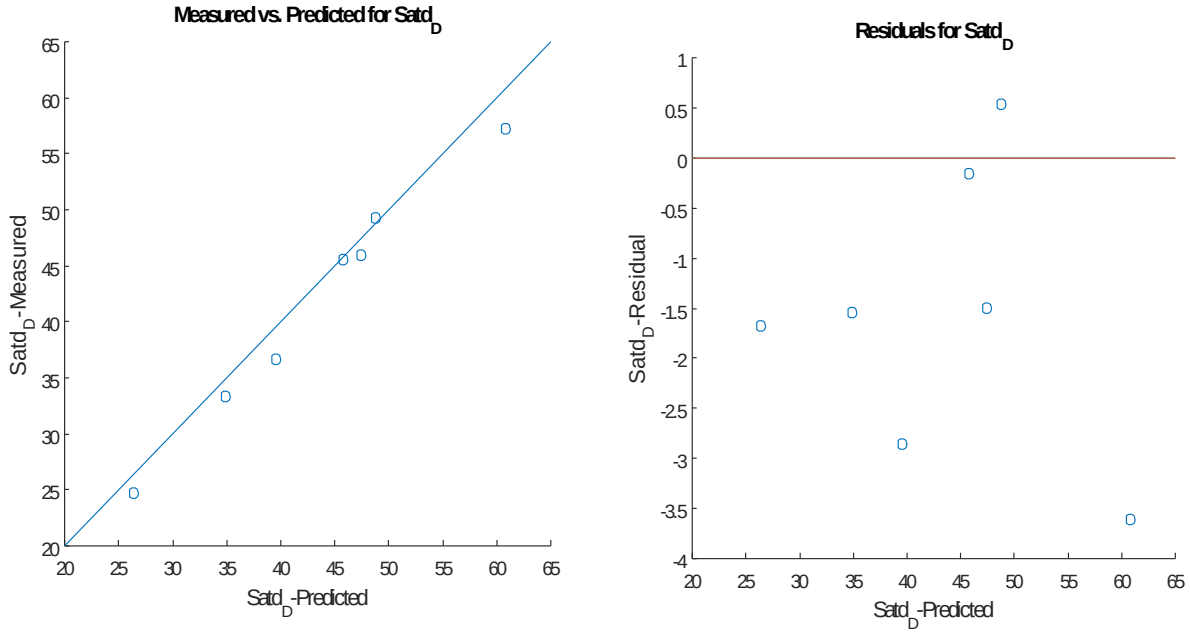

Figure 4: Plots of predicted vs. actual data (LHS) and the residual information (RHS) for saturated content estimation.

Comparing the predicted and actual data, there is a good agreement with each other. The residuals between actual data and the predicted one are varying from around -3.5 to +1 for this testing data.

Model for aromatic content estimation of D

Using the data in Table 1, the linear relationship is investigated between aromatic composition and bulk physical properties via scatter plots as given in Figure 5.

Similar to saturated one, the aromatic content shows a dependence of bulk physical properties d, RI, KV80 and KV100. As SC and CR data are rather scattered compared to the others, these are eliminated from the predictor variables. Besides, the only d is considered again among d and RI. Together with d, the properties KV80, and KV100 are selected as independent variables.

Fitting a linear model with the selected predictor variables, the corresponding p-values listed in Table 4 are checked for their significance. As those for KV80 and KV100 are far higher than 0.05, S estimation with 0.975 of confidence level is applied to determine the outliers.

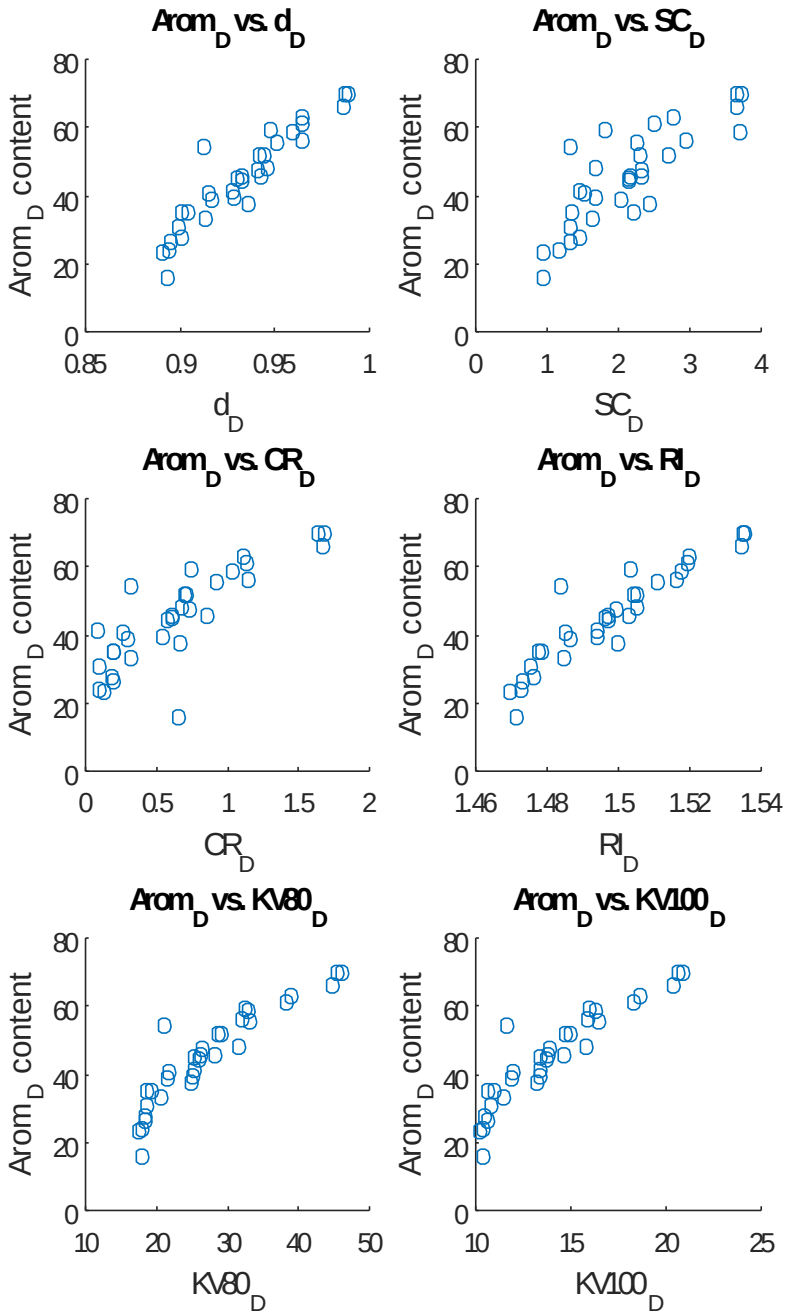

Figure 5: Scatterplots of predictor variable candidates for aromatic content estimation.

The outliers are found to be the 2nd, 3rd, 8th, 13th and 18th rows (18th row is an addition

compared to saturated case). Eliminating these outliers, and using the 75% of remaining data for training, the fitting parameters are found as listed in Table 4.

Table 4: p-values for the selected bulk physical properties as predictor variables for Arom content (Values given for both complete dataset and training dataset without outliers)

	For complete dataset				For dataset without outliers			
Term	**Estimate**	**Std.Er.**	**t Ratio**	**Prob>|t|**	**Estimate**	**Std.Er.**	**t Ratio**	**Prob>|t|**
Intercept	-310.00	142.8	-2.17	0.0386	-273.06	89.10	-3.06	0.0074
d_D	355.83	188.9	1.88	0.0701	294.26	117.6	2.50	0.0235
$KV80_D$	-0.9649	2.738	-0.35	0.7272	-2.1756	1.554	-1.40	0.1805
$KV100_D$	3.5157	8.135	0.43	0.6689	7.2443	4.679	1.55	0.1411

Comparing the p-values given in Table 4, all three parameter estimates are improved by disregarding the outliers. Though the ones for KV80 and KV100 are still higher than 0.05, they are kept as the predictor variables to value their relatively small contribution to the estimation beside the density term (R^2 is improved from 0.969 to 0.973 when viscosity terms are added into the equation.). The corresponding model equation for Aromatic content estimation is given in Eq. (7) together with the summary of fit and ANOVA table below:

$$x_{Arom}^{HND} = -273.06 + 294.26 * d_D - 2.18 * KV80_D + 7.24 * KV100_D \quad \text{(Eq. 7)}$$

RSquare	0.973226
RSquare Adj	0.968206
Root Mean Square Error	2.440678
Mean of Response	42.92
Observations (or Sum Wgts)	20

Source	**DF**	**Sum of Squares**	**Mean Square**	**F Ratio**
Model	3	3464.4766	1154.83	193.8632
Error	16	95.3106	5.96	**Prob > F**
C. Total	19	3559.7872		<.0001*

The model is tested with the remaining data. Putting the predicted and actual data, as well as the residual information in graphs, results in Figure 6.

Comparing the predicted and actual data, there is a good agreement with each other. The residuals between actual data and the predicted one are varying from around +0.5 to +3.5 for this testing data. In other words, the prediction slightly underestimates the testing data.

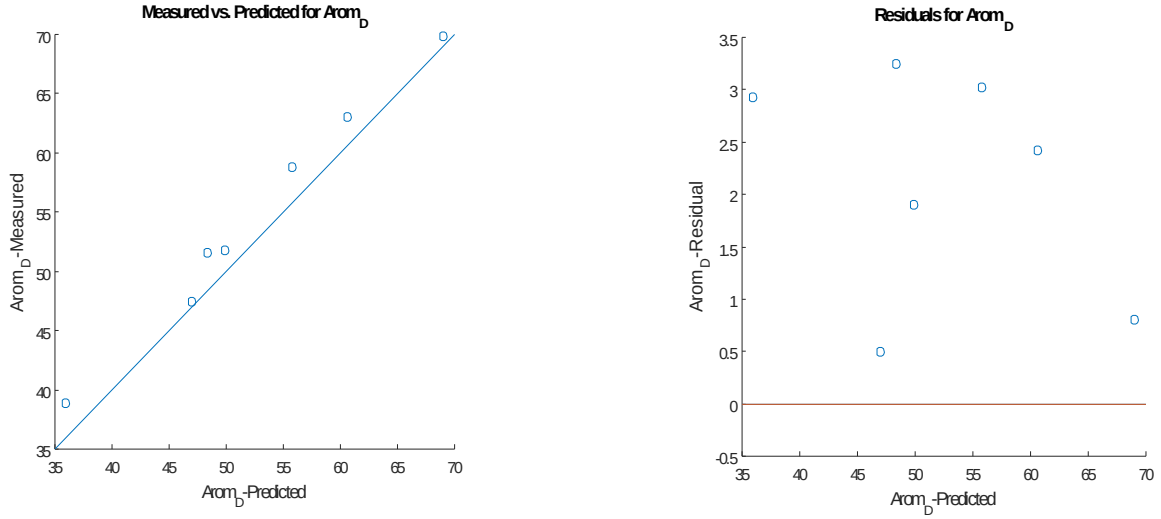

Figure 6: Plots of predicted vs. actual data supplemented (LHS) and the residual information (RHS) for aromatic content estimation.

Model for stage efficiency estimation

Using the data in Table 2, the linear relationship is investigated between stage efficiency and selected operational data via scatter plots as given in Figure 7.

Stage efficiency shows the dependence of the operational information T_S and $F_{S/D}$ with less scattered data compared to the other three variables. F_D can be treated as categorical rather than continuous data. As most of F_D is concentrated into one value for a large range of efficiency, it would not be a significant predictor. Looking at T_D and F_S, they are rather scattered. Therefore, T_S and $F_{S/D}$ are selected as significant variables.

Fitting a linear model with the selected predictor variables, the corresponding p-values listed in Table 5 are checked for their significance. As they are less than 0.05 for both variables, it is approved that they are significant for efficiency estimation. In spite of this, the calculated R^2 is 0.78, which means that only 78% of the efficiency variable is explained by the selected operational variables. It is indeed not sufficient to have results with higher accuracy from the Aspen model. Therefore, S estimation with 0.975 of confidence level is applied to determine the outliers.

The outliers are found to be the 3rd, 14th, 15th and 18th Rows. Eliminating these outliers, and using the 75% of remaining data for training, the fitting parameters are found as listed in Table 5.

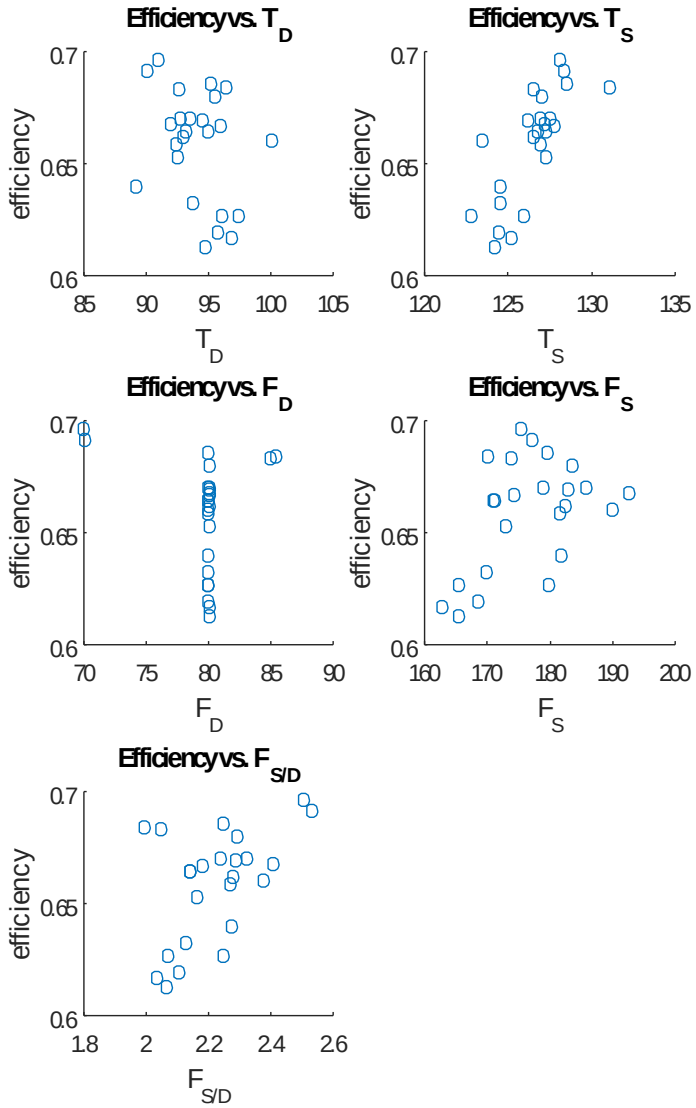

Figure 7: Scatterplots of predictor variable candidates for stage efficiency estimation.

Table 5: p-values for the selected operational data as predictor variables for efficiency (Values given for both complete dataset and the training dataset without outliers)

	For complete dataset				For dataset without outliers			
Term	**Estimate**	**Std.Er.**	**t Ratio**	**Prob>|t|**	**Estimate**	**Std.Er.**	**t Ratio**	**Prob>|t|**
Intercept	-0.7336	0.175	-4.19	0.0004	-0.9867	0.123	-8.03	<.0001
TS	0.0097	0.001	7.01	<.0001	0.0104	0.001	10.1	<.0001
FS/D	0.0771	0.018	4.34	0.0003	0.1486	0.019	7.74	<.0001

Comparing the p-values given in Table 5, disregarding the outliers makes all parameters to be much lower than 0.05. More importantly, R^2 is improved to 0.953). The corresponding model equation for stage efficiency estimation is given in Eq. (8) together with the summary of fit and ANOVA table below:

$$\varepsilon = -0.99 + 0.01 * T_S + 0.15 * F_{S/D} \quad \text{(Eq. 8)}$$

RSquare	0.952703
RSquare Adj	0.944821
Root Mean Square Error	0.005819
Mean of Response	0.65
Observations (or Sum Wgts)	15

Source	**DF**	**Sum of Squares**	**Mean Square**	**F Ratio**
Model	2	0.00818563	0.004093	120.8589
Error	12	0.00040637	0.000034	**Prob > F**
C. Total	14	0.00859200		<.0001*

The model is tested with the remaining data. Putting the predicted and actual data, as well as the residual information in graphs, results in Figure 8.

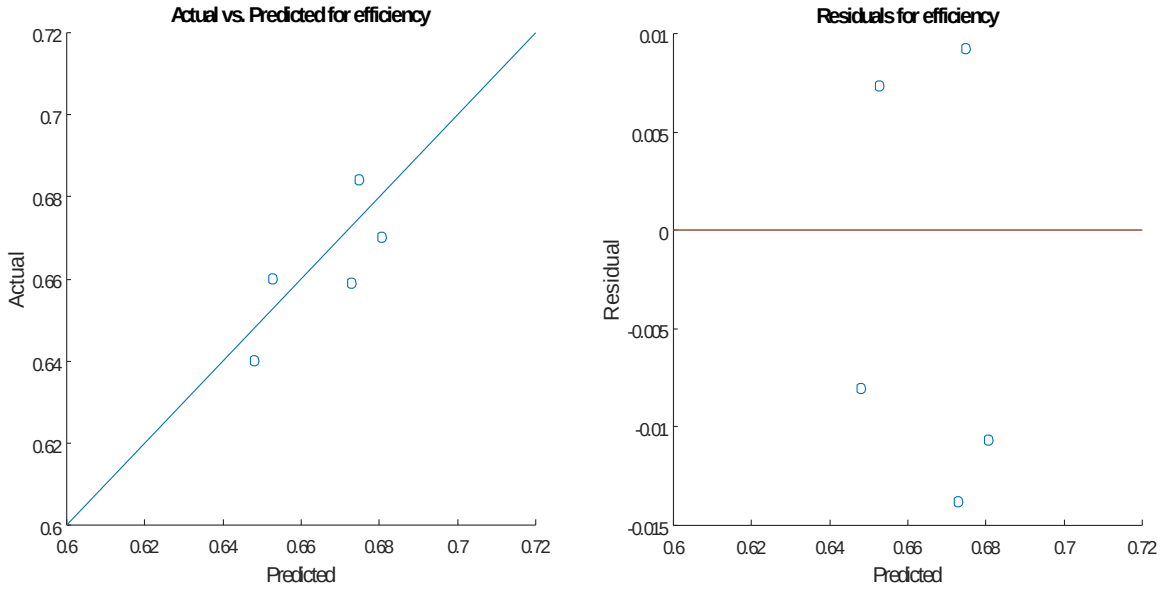

Figure 8: Plots of predicted vs. actual data (LHS) and the residual information (RHS) for stage efficiency estimation.

Comparing the predicted and actual data, there is a good agreement with each other. The residuals between actual data and the predicted one are varying from around -0.015 to +0.01 for this testing data.

Model for raffinate VI estimation

Using the data in Table 2, the linear relationship between VI_R and compositional data calculated for R by Aspen model is investigated via scatter plots, as given in Figure 9.

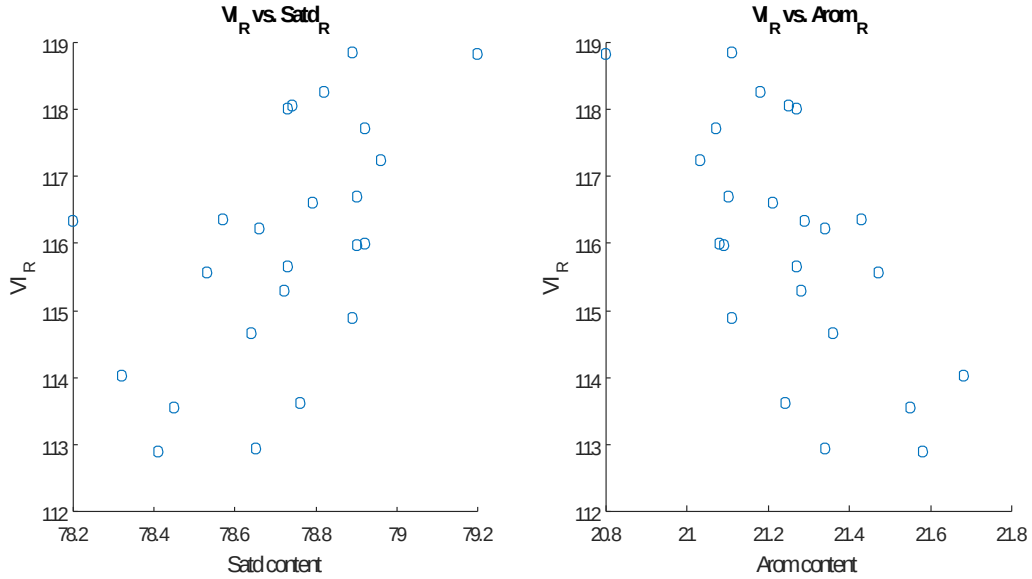

Figure 9: Scatterplots of predictor variable candidates ($Satd_R$ & $Arom_R$) for VI_R estimation.

Looking through the available data, the component values have a range of 1%, while VI_R changes in a range of 6%. Besides, the dependency is somewhat scattered.

Fitting a linear model with both saturated and aromatic contents as predictor variables, the corresponding p-values are given in Table 6. Among them, the one for aromatic content is less than 0.05, so it is kept as a predictor, while saturated content is disregarded. Here it is important to note that the calculated R^2 is only 0.44. There is also some difference between R^2 and adjusted R^2 (=0.39).

S estimation with 0.975 of confidence level is applied, but no outliers are detected with this confidence level. Using the 75% of the whole data for training, the fitting parameters are found as listed in Table 6.

Table 6: p-values for the compositional data as predictor variables for VI_R (Values given for both complete and training datasets)

	For complete dataset				**For dataset without outliers**			
Term	**Estimate**	**Std.Er.**	**t Ratio**	**Prob>|t|**	**Estimate**	**Std.Er.**	**t Ratio**	**Prob>|t|**
Intercept	344.72	284.7	1.21	0.2395	240.98	33.15	7.27	<.0001
x^R_{Satd}	-1.0152	2.820	-0.36	0.7225	0	-	-	-
x^R_{Arom}	-7.0000	3.227	-2.17	0.0417	-5.8882	1.560	-3.77	0.0017

Comparing the p-values given in Table 6, taking only the aromatic content as predictor improves the p-values. The corresponding model equation for VI_R estimation is given in Eq. (9) along with the summary of fit and ANOVA table below:

RSquare	0.470954
RSquare Adj	0.437889
Root Mean Square Error	1.264623
Mean of Response	115.8776
Observations (or Sum Wgts)	18

$$VI_R = 240.98 - 5.89 * x^R_{Arom} \quad \text{(Eq. 9)}$$

Source	**DF**	**Sum of Squares**	**Mean Square**	**F Ratio**
Model	1	22.778615	22.7786	14.2431
Error	16	25.588351	1.5993	**Prob > F**
C. Total	17	48.366966		0.0017*

Here, R^2 is improved a bit from 0.44 to 0.47 by using only aromatic content as predictor, but it is not enough to treat this model as a reliable one. This low accuracy could be originated even from the lab measurements for VI_R calculation. According to the corresponding viscosity measurement standard EN ISO 3104, the reproducibility tolerates an error of 0.65%. In the case that one viscosity value is with -0.65% error

in measurement while the other one is with +0.65% error, the calculated VI (according to ASTM D2270 standard) would have an error of about 10%. For example, the VI_R calculated from the measured KV80 and KV100 for the 20. test-run is around 113, and this can be changed from 104 to 124 by taking the error tolerance into account. Indeed, this 10% error covers the VI_R range specific to the test-run. Therefore, the equation is used as indicative, but not for decision making in operation.

In spite of low prediction power, the model is tested with the remaining data. Putting the predicted and actual data, as well as the residual information in graphs, results in Figure 10: Comparing the predicted and actual data, they are in line with each other. The residuals between actual data and the predicted one are varying from around -2.5 to +2.5 for this testing data.

Results of Yield and VI estimations via using complete model

The input and output data used for estimating Y_R and VI_R values via the complete model are given in Table 7. The measured bulk physical properties (d, KV80 and KV100) are used to calculate the composition of D, which is the input to the Aspen model. From the operational data (T_S and $F_{S/D}$), ε is found and it is again used in the Aspen model. The composition and flow rate information of R taken from the Aspen model are compared with the realized VI_R (via the lab measurements) and yield data (via the measured plant data). It is seen that data 1 & 18 for VI_R and Y_R are rather deviated from the corresponding realized ones, while the others are more in line with the real data.

Then, the predicted R_F appears to have deviated from the realized R_F at a value of -35.1%. Reminding that data 18 is determined as an outlier and disregarded during model construction for stage efficiency, such deviation in the predicted values corresponding to this data is reasonable. Comparing the data for row 18 with 17, the physical properties of HND (d_D, $KV80_D$ and $KV100_D$) are quite close to each other. It is an expected result for feed properties, as 18. Run is indeed subsequent to 17 within the same operational day. The operational data used for ε prediction are slightly different which causes a difference in the value of ε. However, these differences would not cause such deviation in the prediction power of i.e. Y_R for run 18 compared to 17. In fact, it is the result of fluctuation in the realized raffinate flow of run 18, as seen from Figure 11. The interquartile of F_R is wider for run 18. With whisker length being 1.0 times the interquartile range, there are 3 outliers for run 18, while there is only one for run 17. This results in higher average R_F and so higher reconciliation efficiency value than it should be for data 18.

The other deviated one, data 1, is indeed not used in model construction at all. It remained in the testing part, so its deviation is detected at this later stage. Looking through the details from Table 7, the physical properties and composition data are in line with each other. However, as it is seen from Figure 12, there is a fluctuation especially in F_S and T_S at the time span between 40 and 60. This causes deviation in the average values of F_S and T_S which are used in ε prediction. Eventually, it brings the corresponding error in the predicted Y_R value.

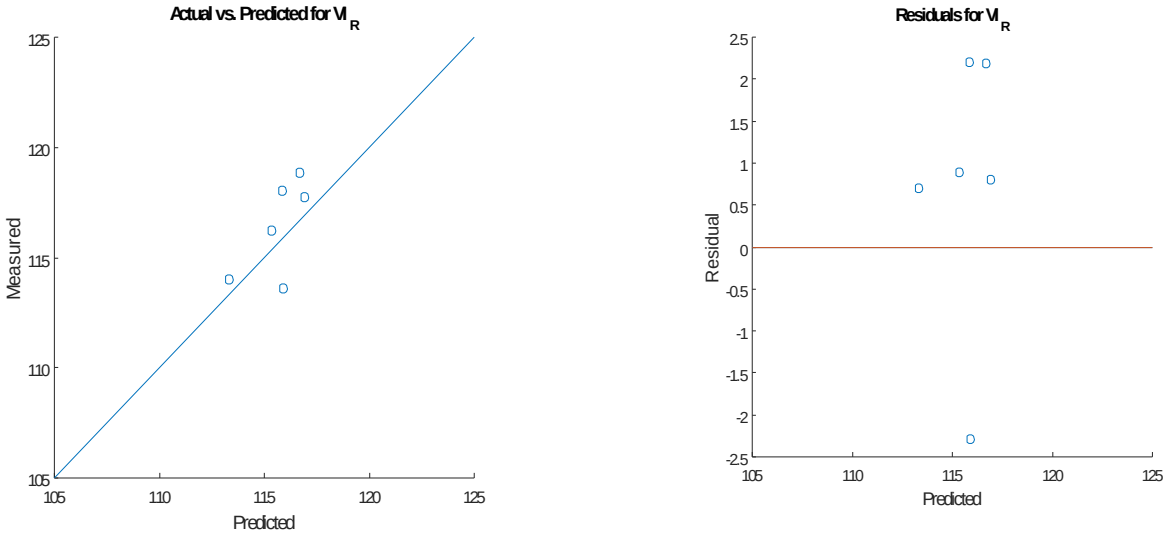

Figure 10: Plots of Predicted vs. actual data (LHS) and the residual information (RHS) for VI_R estimation.

Table 9: The realized operational & experimental data and model results for the additional test-runs

Lab measurements			**Model**		**Op. data**		**ε**	**Model**		**VI_R**			**Y_R**		
d_D	**$KV80_D$**	**$KV100_D$**	**$Satd_D$**	**$Arom_D$**	**T_S**	**$F_{S/D}$**	**Model**	**$Satd_R$**	**$Arom_R$**	**ASTM**	**Model**	**Error%**	**Op.**	**Model**	**Error%**
0.936	25.40	13.40	51.99	44.09	122.69	2.16	0.612	78.12	21.88	108.7	112.1	3.2	0.51	0.47	-7.7
0.935	25.24	13.33	52.49	43.64	126.03	2.16	0.647	78.28	21.71	110.5	113.1	2.4	0.48	0.47	-3.8
0.935	25.40	13.41	52.20	43.90	126.70	2.13	0.650	78.30	21.70	110.3	113.2	2.6	0.46	0.47	2.8
0.938	25.98	13.60	50.95	45.07	124.62	2.21	0.639	78.42	21.58	108.9	113.9	4.6	0.42	0.46	8.0
0.939	25.99	13.57	51.15	44.93	125.63	2.19	0.647	78.27	21.73	112.4	113.0	0.5	0.43	0.48	11.9
0.940	26.23	13.68	50.32	45.67	125.70	2.22	0.653	78.72	21.28	115.1	115.7	0.5	0.40	0.42	4.9
0.940	26.14	13.63	50.71	45.33	125.94	2.24	0.658	78.51	21.49	110.7	114.4	3.4	0.41	0.42	4.6
0.940	26.23	13.67	50.41	45.60	127.12	2.28	0.676	78.85	21.15	113.0	116.4	3.0	0.37	0.42	12.0
0.940	26.10	13.62	50.48	45.52	127.13	2.31	0.681	78.68	21.32	114.0	115.4	1.3	0.37	0.43	16.6

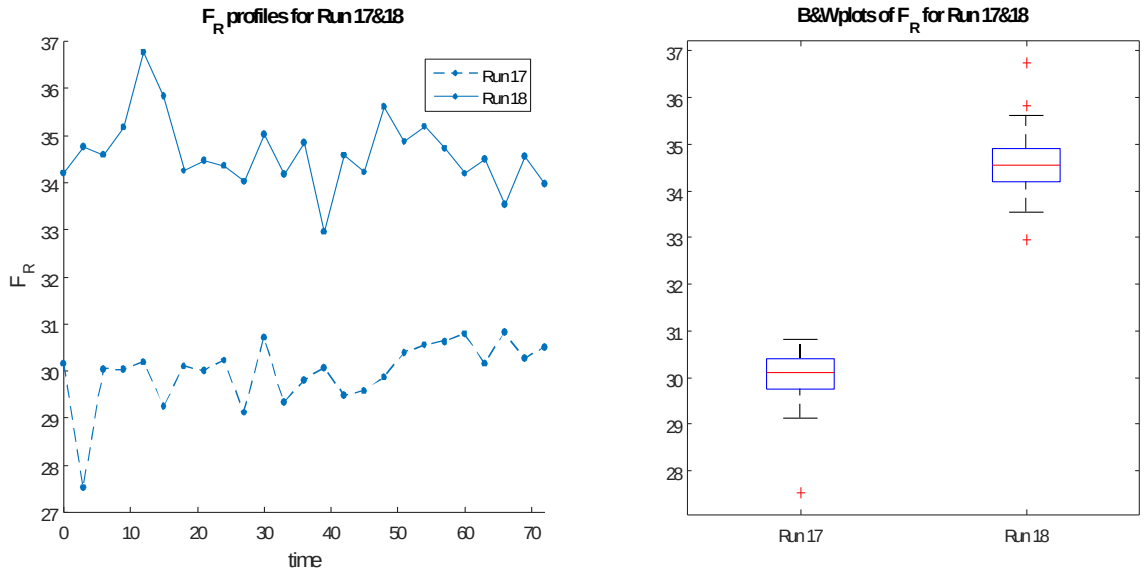

Figure 11: Plots of F_R profiles in a timespan (LHS) and Box & Whisker (RHS) corresponding to Run 17 & 18.

Table 7: Input and output data for model estimation of VI_R and Y_R

	Lab measurements					Model		Op. data	ε	Model	VI_R			Y_R		
TR#	**d_D**	**$KV80_D$**	**$KV100_D$**	**$Satd_D$**	**$Arom_D$**	**TS**	**$F_{S/D}$**	**Model**	**$Satd_R$**	**$Arom_R$**	**ASTM***	**Model**	**Error%**	**Op.**	**Model**	**Error%**
1	0.936	25.55	13.37	52.53	43.70	131.06	1.99	0.675	78.90	21.09	116.0	119.7	3.2	0.33	0.23	-31.3
2	0.938	25.72	13.52	51.06	44.94	126.95	2.32	0.681	78.92	21.07	117.7	117.3	-0.4	0.37	0.41	9.4
3	0.938	25.58	13.42	51.49	44.58	127.19	2.41	0.696	78.89	21.11	118.9	116.4	-2.1	0.37	0.43	18.6
4	0.939	25.74	13.55	50.61	45.32	124.49	2.27	0.648	78.90	21.10	116.7	116.1	-0.5	0.38	0.41	6.2
5	0.939	25.54	13.39	51.48	44.60	123.48	2.38	0.653	78.73	21.27	118.0	115.7	-1.9	0.44	0.43	-2.6
6	0.939	25.81	13.50	51.06	44.98	126.93	2.27	0.673	78.92	21.08	116.0	115.6	-0.3	0.40	0.43	9.9
7	0.939	25.86	13.52	51.03	45.02	126.20	2.28	0.667	78.82	21.18	118.3	116.9	-1.2	0.41	0.40	-1.4
8	0.940	26.08	13.61	50.78	45.25	127.48	2.24	0.674	78.20	21.29	116.3	115.9	-0.3	0.38	0.40	4.0
9	0.940	26.15	13.64	50.68	45.35	127.28	2.16	0.660	78.76	21.24	113.6	114.6	0.8	0.40	0.42	5.6
10	0.938	26.21	13.67	50.99	45.08	126.49	2.28	0.669	78.72	21.28	115.3	115.6	0.3	0.39	0.41	5.1
11	0.939	26.12	13.66	50.62	45.38	127.01	2.29	0.677	78.89	21.11	114.9	116.6	1.4	0.40	0.40	-1.2
12	0.939	26.20	13.67	50.66	45.37	127.79	2.18	0.668	78.79	21.21	116.6	117.2	0.5	0.37	0.37	1.9
13	0.939	26.15	13.65	50.69	45.33	128.52	2.25	0.686	78.73	21.27	115.7	115.7	0.0	0.40	0.40	0.4
14	0.940	26.15	13.68	50.12	45.81	128.31	2.53	0.726	79.20	20.80	118.8	116.2	-2.2	0.39	0.45	16.0
15	0.940	26.22	13.69	50.20	45.76	128.08	2.51	0.720	78.96	21.03	117.2	115.7	-1.2	0.41	0.45	10.2
16	0.938	25.66	13.50	51.23	44.78	126.79	2.14	0.652	78.66	21.34	116.2	117.6	1.2	0.39	0.33	-16.1
17	0.937	25.72	13.51	51.52	44.55	127.25	2.14	0.656	78.74	21.25	118.1	118.4	0.3	0.38	0.34	-10.3
18	0.937	25.75	13.67	50.19	45.61	126.51	2.05	0.635	78.65	21.34	112.9	117.6	4.1	0.41	0.26	-35.1
19	0.938	25.55	13.44	51.29	44.73	124.54	2.12	0.626	78.57	21.43	116.4	114.3	-1.8	0.42	0.40	-4.4
20	0.938	25.60	13.46	51.18	44.83	124.16	2.07	0.613	78.45	21.55	113.5	114.1	0.5	0.41	0.40	-0.1
21	0.936	25.04	13.22	52.44	43.69	124.41	2.11	0.622	78.53	21.47	115.6	113.9	-1.5	0.42	0.43	2.0
22	0.936	25.04	13.22	52.37	43.75	122.77	2.25	0.626	78.41	21.58	112.9	114.0	0.9	0.45	0.45	-0.5
23	0.936	24.97	13.18	52.53	43.61	125.22	2.04	0.620	78.32	21.68	114.0	113.7	-0.3	0.42	0.43	2.9
24	0.937	25.12	13.24	52.32	43.81	125.90	2.07	0.632	78.64	21.36	114.7	114.4	-0.3	0.40	0.42	4.4

* According to ASTM D2270

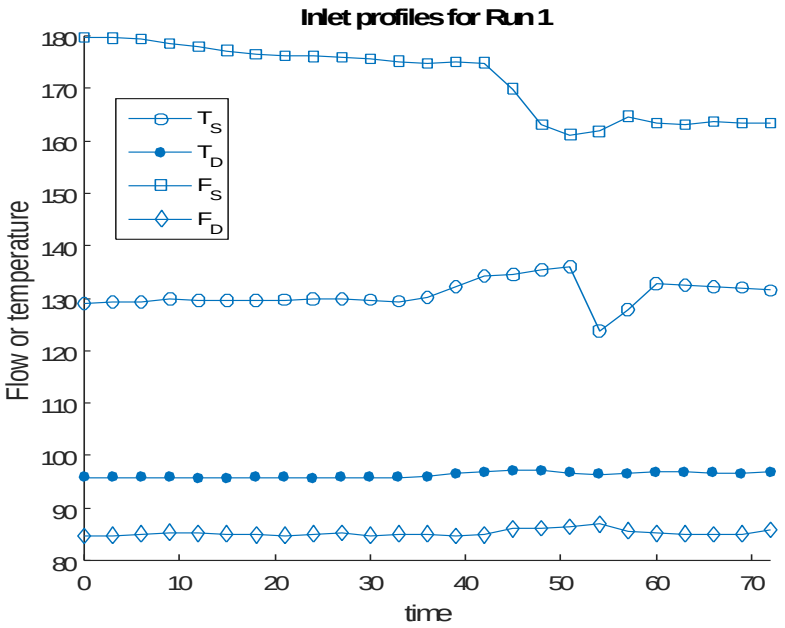

Figure 12: Operational profiles in a timespan corresponding to Data 1.

Along with data 1 and 18, RMSE is calculated to be 1.7 and 0.047 for VI_R and Y_R, respectively. Extracting these 2 outliers, the RMSE decreases to 1.3 and 0.031, respectively. These values are at acceptable levels, so the model can be used for prediction of VI_R and Y_R via using only the measured bulk physical properties of distillate together with the operational data already available in the plant historian. In addition to that, Y_R prediction can be used for decisive actions, such as tuning of operating conditions and profit maximization.

Estimating ε from the selected inlet operating conditions gives higher accuracy of model compared to use of a constant value for all operating conditions. The results are given for comparison in Table 8. Here, the constant value of ε is taken as the average of reconciliations from Table 2. The rows belonging to Run 1 and 18 are extracted from this table. Calculating the RMSE values for both the model predicted F_R's and those found by keeping ε constant at 0.658, they are found as 2.4 and 6.0, respectively. This shows that the power of prediction increases when the hydraulic changes are taken into account at each run.

Table 8: The realized and model predicted F_R values beside the calculated F_R with constant ε

TR#	F_R (realized)	F_R (model)	Error%*	F_R (ε=0.658)	Error%**
2	29.64	32.43	9.4	25.91	-12.6
3	29.24	34.69	18.6	26.27	-10.2
4	30.47	32.36	6.2	34.36	12.8
5	35.12	34.22	-2.6	34.85	-0.8
6	31.57	34.68	9.9	31.53	-0.1
7	32.58	32.11	-1.4	30.10	-7.6
8	30.72	31.93	4.0	27.13	-11.7
9	32.01	33.79	5.6	33.22	3.8
10	31.44	33.05	5.1	30.46	-3.1
11	32.04	31.65	-1.2	26.04	-18.7
12	29.34	29.91	1.9	26.52	-9.6
13	31.97	32.09	0.4	23.04	-27.9
14	27.22	31.56	16.0	19.89	-26.9

15	28.60	31.51	10.2	21.00	-26.6
16	31.35	26.30	-16.1	29.34	-6.4
17	30.09	27.00	-10.3	27.75	-7.8
19	33.65	32.15	-4.4	38.47	14.3
20	32.41	32.38	-0.1	40.45	24.8
21	33.83	34.50	2.0	40.64	20.1
22	36.19	36.03	-0.5	40.71	12.5
23	33.31	34.27	2.9	41.45	24.5
24	32.03	33.43	4.4	38.88	21.4

* Corresponding to the model calculated efficiency
** Corresponding to the constant value of efficiency

A second validation is performed for the model by conducting an additional series of test-runs at the existing unit. The realized operational and experimental data together with the model results are given in Table 9. Accordingly, the percent errors for Y_R vary between -7.7 and 16.6, while those for VI_R are up to 14%. The plots of predicted vs. realized data and the residuals are also given in Figures 13 & 14.

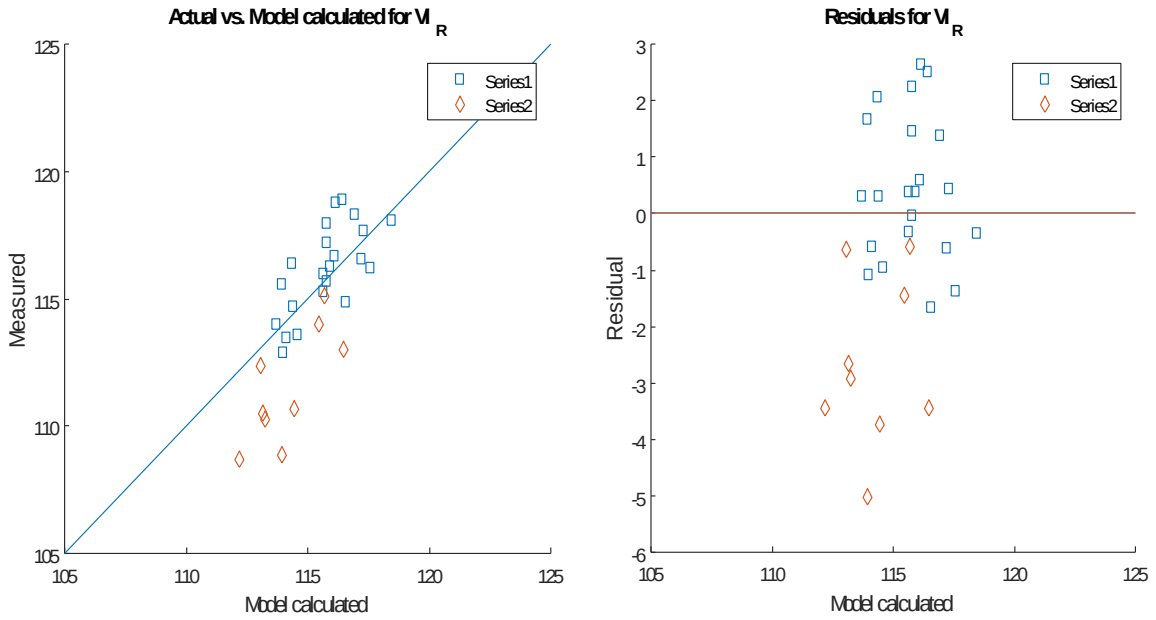

Figure 13: Plots of predicted vs. realized data (LHS) and the residuals (RHS) for VI_R prediction.

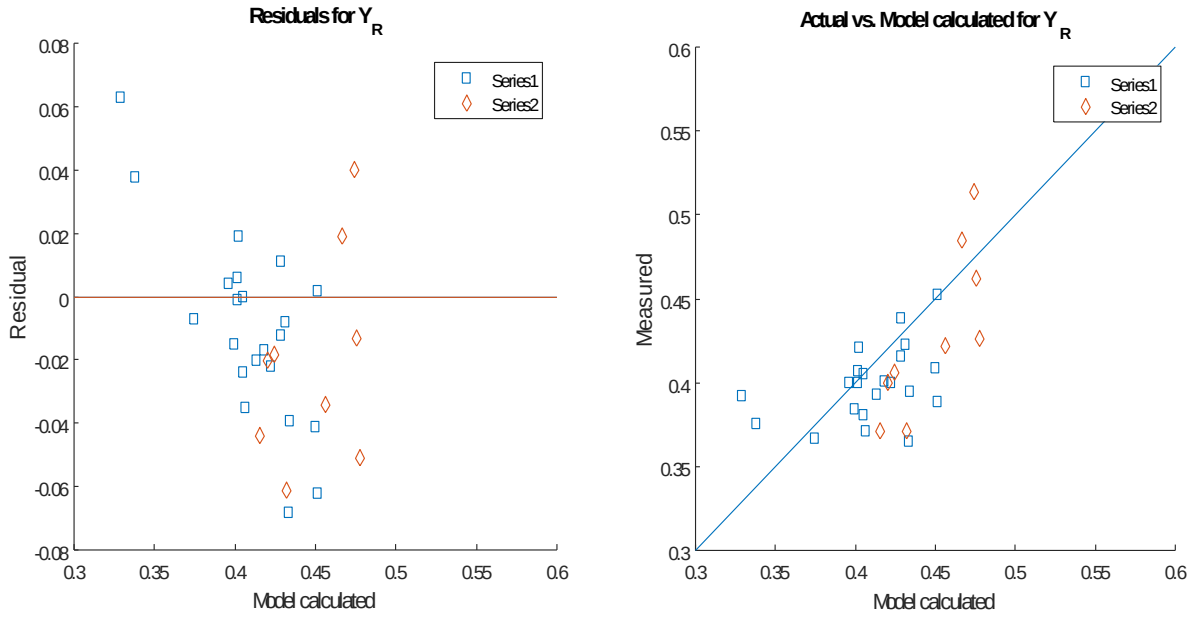

Figure 14: Plots of predicted vs. realized data (LHS) and the residuals (RHS) for Y_R prediction.

The model overpredicts VI_R values for this dataset. The RMSE for VI_R values is calculated as 3. Referring to the previously stated uncertainty in VI values originated from the lab measurements, these results prove that VI_R prediction should be kept as the indication only. For Y_R, RMSE is 0.04, which is an acceptable level.

CONCLUSION

The test-runs conducted in the existing lube base oil unit validate that Aspen process model supported with a regression model for stage efficiency has a higher accuracy compared to the one for which the efficiency is a constant value. This shows that the prediction power can be increased by taking the hydraulic changes into account at each run.

The published phase equilibrium data for Heavy Neutral Distillate + Furfural system is used for constructing the industrial-scale extraction process model in Aspen Hysys. Here, the distillate is composed of three pseudo-components; namely saturated, aromatic and polar. The compositional data (as an input of feed stream in the process model) is determined from the bulk physical properties of distillate. Applying multiple regression techniques to the laboratory data, density as well as kinematic viscosity at 80 and 100 °C are found to be significant predictors for saturated and aromatic compositions. Refractive index shows significance but it is highly correlated with density as well. Sulfur content and carbon residue values are rather scattered considering the measured values of compositions.

As another input for Aspen model, the stage efficiency is calculated from the operating conditions. Analyzing the corresponding test-run data, the solvent temperature and solvent-to-distillate ratio have significance for predicting the efficiency value.

Raffinate yield and VI are the key performance parameters for the extraction process. Raffinate flow rate and composition data is available as Aspen model output. Yield is calculated as raffinate-to-distillate flow ratio. To obtain VI value, the composition data from Aspen model is converted into VI via a statistical model which is constructed by using test-run data from the existing plant. As the composition data used for model construction has a narrow range (1%), the VI prediction can be used for only indication. On the other hand, yield prediction has a fair accuracy with relative error changing between -16 to +19%, and it can be used for decision making by the corresponding process and planning teams of the refinery.

ACKNOWLEDGMENTS

This work was partially supported by Scientific and Technological Research Council of Turkey grant funded by Turkish government (TEYDEP project number: 3130749).

NOMENCLATURE

A_0: Intercept term for estimation of stage efficiency

$A_{0,Arom}^{HND}$: Intercept term for aromatic content estimation

$A_{0,satd}^{HND}$: Intercept term for saturated content estimation
$A_{j,Arom}^{HND}$: The parameter of the jth physical property of HND for aromatic content
$A_{j,satd}^{HND}$: The parameter corresponding to the jth physical property of HND
A_k : The parameter of the kth operational data of extraction process
Arom: Aromatic content
BLO: Base Lube Oil
BS: Bright Stock
CR: Carbon Residue
d: Density@15C
D: Distillate
ε: Stage efficiency
E_mix: Extract mixed with Solvent
F: Operational flowrate
FEU: Solvent (Furfural) Extraction Unit
HN: Heavy Neautral
HND: Heavy Neutral Distillate
KV40: Kinematic viscosity at 40C
KV80: Kinematic viscosity at 80C
KV100: Kinematic viscosity at 100C
LN: Light Neutral
O_k: The kth operational data of extraction process
P_j^{HND} : The jth physical property of HND
PDU: Propane Deasphalting Unit
R: Raffinate
R_mix: Raffinate mixed with Solvent
RDC: Rotating Disc Column
RI: Refractive Index
RMSE: Root Mean Square Error
S: Aromatic extracting solvent
Satd: saturated content
SC: Sulfur content
SO: Spindle Oil
T: Operational temperature
VDU: Vacuum Distillation Unit
VI: Viscosity Index
x_{Arom}^{HND}: Aromatic content of HND in mass percentage
x_{Satd}^{HND}: Saturated content of HND in mass percentage
Y: Yield

REFERENCES

1. Espada JJ, Coto B, Romero R van, Moreno JM. Simulation of pilot-plant extraction experiments to reduce the aromatic content from lubricating oils. Chemical Engineering and Processing. 2008;(47):1398–403.

2. Coto B, Grieken R van, Pena JL, Espada JJ. A model to predict physical properties for light lubricating oils and its application to the extraction process by furfural. Chemical Engineering Science. 2006;(61):4381–92.

3. Coto B, Grieken R van, Pena JL, Espada JJ. A generalized model to predict the liquid-liquid equilibrium in the systems furfural + lubricating oils. Chemical Engineering Science. 2006;(61):8028–39.

4. Grieken R van, Coto B, Romero E, Espada JJ. Prediction of Liquid-Liquid Equilibrium in the System Furfural + Heavy Neutral Distillate Lubricating Oil. 2005;(44):8106–12.

5. Grieken R van, Coto B, Pena JL, Espada JJ. Application of a generalized model to the estimation of physical properties and description of the aromatic extraction from a highly paraffinic lubricating oil. Chemical Engineering Science. 2008;(63):711–20.

6. Espada JJ, Coto B, Pena JL. Liquid-liquid equilibrium in the systems furfural + light lubricating oils using UNIFAC. Fluid Phase Equilibria. 2007;(259):201–9.

7. Pashikanti K, Liu YA. Predictive Modeling of Large-Scale Integrated Refinery Reaction and Fractionation Systems from Plant Data. Part 3: Continuous Catalyst Regeneration (CCR) Reforming Process. Energy Fuel. 2011;(25):5320–44.

8. Albahri TA. Molecularly Explicit Characterization Model (MECM) for Light Petroleum Fractions. Ind Eng Chem Res. 2005;(44):9286–98.

9. Ferreira MC, Meirelles AJA, Batista EAC. Study of the Fusel Oil Distillation Process. Ind Eng Chem Res. 2013;(52):2336–51.

10. Yang C, Yang S, Qian Y, Guo J, Chen Y. Simulation and Operation Cost Estimate for Phenol Extraction and Solvent Recovery Process of Coal-Gasification Wastewater. Ind Eng Chem Res. 2013;(52):12108–15.

11. Muhammad A, GadelHak Y. Correlating the additional amine sweetening cost to acid gases load in natural gas using Aspen Hysys. J of Natural Gas Sci and Eng. 2014;(17):119–30.

12. Maldonado EQ, Meindersma GW, Haan AB. Ionic liquid effects on mass transfer efficiency in extractive distillation of water-ethanol mixtures. Computers and Chemical Engineering. 2014;(71):210–9.

13. Singh D, Gupta RK, Kumar V. Simulation of a plant scale reactive distillation column for esterification of acetic acid. Computers and Chemical Engineering. 2015;(73):70–81.

14. Mehrkesh A, Tavakoli T, Hatamipour MS, Karunanithi T. Modeling and Simulation of a Rotating-Disk Contactor for the Extraction of Aromatic Hydrocarbons from a Lube-Oil Cut. Ind Eng Chem Res. 2013;(52):9422–32.
15. IP 336/04: Petroleum products – Determination of sulfur content – Energy-dispersive X-ray fluorescence spectrometry (ISO 8754:2003). CEN; 2014.

16. ASTM D4530-11: Standard Test Method for Determination of Carbon Residue (Micro Method). ASTM International; 2011.

17. TS 1013 EN ISO 3675: Crude petroleum and liquid petroleum products – Laboratory determination of density or relative density – Hydrometer method. TSE; 2002.

18. ASTM D1218-12: Standard Test Method for Refractive Index and Refractive Dispersion of Hydrocarbon Liquids. ASTM International; 2016.

19. TS 1451 EN ISO 3104: Petroleum products – Transparent and opaque liquids – Determination of kinematic viscosity and calculation of dynamic viscosity (ISO 3104). TSE; 1999.

20. ASTM D2007-11: Standard test method for Characteristic Groups in Rubber Extender and Processing Oils and Other Petroleum-Derived Oils by the Clay-Gel Absorption Chromatographic Method. ASTM International; 2011.

21. ASTM D2270-10: Standard Practice for Calculating Viscosity Index from Kinematic Viscosity at 40°C and 100°C. ASTM International; 2009.

22. ASTM D341-09: Standard Practice for Viscosity-Temperature Charts for Liquid Petroleum Products. ASTM International; 2009.